Accurate determination of an alkali-vapor-inert-gas diffusion coefficient using coherent transient emission from a density grating

Pouliot, Alexander, Carlse, Gehrig, Vacheresse, Thomas, Kumarakrishnan, Anantharaman

Alexander Pouliot, Gehrig Carlse, Thomas Vacheresse, Anantharaman Kumarakrishnan, "Accurate determination of an alkali-vapor-inert-gas diffusion coefficient using coherent transient emission from a density grating," Proc. SPIE 12016, Optical and Quantum Sensing and Precision Metrology II, 120160Q (2 March 2022); doi: 10.1117/12.2616878

SPIE.

Event: SPIE OPTO, 2022, San Francisco, California, United States

Accurate determination of an alkali-vapor–inert-gas diffusion coefficient using coherent transient emission from a density grating

Alexander Pouliot, Gehrig Carlse, Thomas Vacheresse and Anantharaman Kumarakrishnan*
York University, Department of Physics and Astronomy, Toronto ON, M3J 1P3

ABSTRACT

We demonstrate a technique for the accurate measurement of diffusion coefficients for alkali vapor in an inert buffer gas. The measurement was performed by establishing a spatially periodic density grating in isotopically pure ^{87}Rb vapor and observing the decaying coherent emission from the grating due to the diffusive motion of the vapor through N_2 buffer gas. We obtain a diffusion coefficient of 0.245 ± 0.002 cm^2/s at 50°C and 564 Torr. Scaling to atmospheric pressure, we obtain $D_0 = 0.1819 \pm 0.0024$ cm^2/s. To the best of our knowledge, this represents the most accurate determination of the Rb-N_2 diffusion coefficient. Our measurements can be extended to different buffer gases and alkali vapors used for magnetometry and can be used to constrain theoretical diffusion models for these systems.
Keywords: Atomic coherences, Magnetometry, Diffusion, Coherent transient effects, Coherence gratings, Diode lasers

1. INTRODUCTION

We have relied on the successful development of a new class of low cost, homebuilt auto-locking laser systems (ALS)[1] to realize experiments in precision metrology that rely on the intrinsic sensitivity of atoms and the advantages of coherent transient techniques. ALS consist of vacuum-sealed, continuous wave (cw) diode lasers that can be frequency stabilized or scanned with respect to atomic, molecular, and temperature tunable frequency markers without human intervention using a digital controller that uses a variety of algorithms[1,2]. This paper describes the most accurate measurement of a diffusion coefficient for an alkali atom in a nitrogen buffer gas environment, a measurement which plays a central role in the design of atomic magnetometers[3].

1.1 Motivation

Spin-Exchange Relaxation–Free (SERF) atomic vapor magnetometers have leapfrogged superconducting sensors to become the most sensitive devices for measuring small magnetic fields and magnetic anomalies[4]. Such devices operate by optically pumping alkali vapor such as rubidium, into a specific internal state, thereby creating a macroscopic magnetic dipole moment that oscillates at the Larmor frequency, ω_L, associated with the external magnetic field. In a conventional time-domain magnetometer, ω_L is measured by observing the absorption of a weak probe laser[5]. SERF magnetometers achieve high precision by preserving the alignment of dipoles over extended time scales using high alkali densities and specific concentrations of buffer gases and quenching gases so that the optically pumped vapor diffuses slowly without decoherence due to radiation trapping and spin exchange collisions. Vapor cell magnetometers are used for the non-invasive exploration of metal and mineral deposits through large area aircraft borne surveys. Since these devices require large vapor densities and correspondingly high laser power (several Watts) for optical pumping, identifying the best configurations and realizing accurate measurements of diffusion coefficients to model magnetometer performance remain critical challenges. These coefficients are also necessary for understanding the dynamics of high-resolution biomedical imaging using spin-polarized noble gases[6], testing collision models based on interatomic potentials[7], and for monitoring the Earth's Ocean currents and interior dynamics using mesospheric sodium vapor magnetometry[8].

2. METHODOLOGY

We have investigated a distinctive coherence magnetometer (CM) that can detect magnetic fields with potentially larger signal strengths than traditional magnetometers[9-12]. CMs detect the evolution of atomic coherences that produce spatially periodic superpositions of atomic states. They produce coherent bursts containing Larmor oscillations along specific directions (due to phase matching) that can be detected over a larger dynamic range than probe transmission.

*akumar@yorku.ca; datamac.phys.yorku.ca

Optical and Quantum Sensing and Precision Metrology II, edited by
Jacob Scheuer, Selim M. Shahriar, Proc. of SPIE Vol. 12016, 120160Q
 · 0277-786X · doi: 10.1117/12.2616878

Here, two laser pulses, overlapped at a small angle θ, create a transverse coherence grating (see Fig. 1). This angle defines the spacing between grating planes. When one of the pulses is turned on, the signal scattered from the grating along the other beam direction decays due to the diffusion of atoms between the planes.

In this work, we have exploited the long-lived decay of a magnetic field insensitive density grating that has the same spatial period as the coherence grating[13]. By measuring the decay time and its characteristic $1/\theta^2$ dependence in isotopically pure ^{87}Rb vapor and nitrogen buffer gas enclosed in a sealed glass cell, we have obtained the most accurate Rb diffusion coefficient in such an environment. This measurement also relied on spectroscopy of pressure broadened resonances to determine the buffer gas concentration. Examples of complementary studies in the frequency domain include the work in Ref. 14.

3. THEORETICAL BACKGROUND

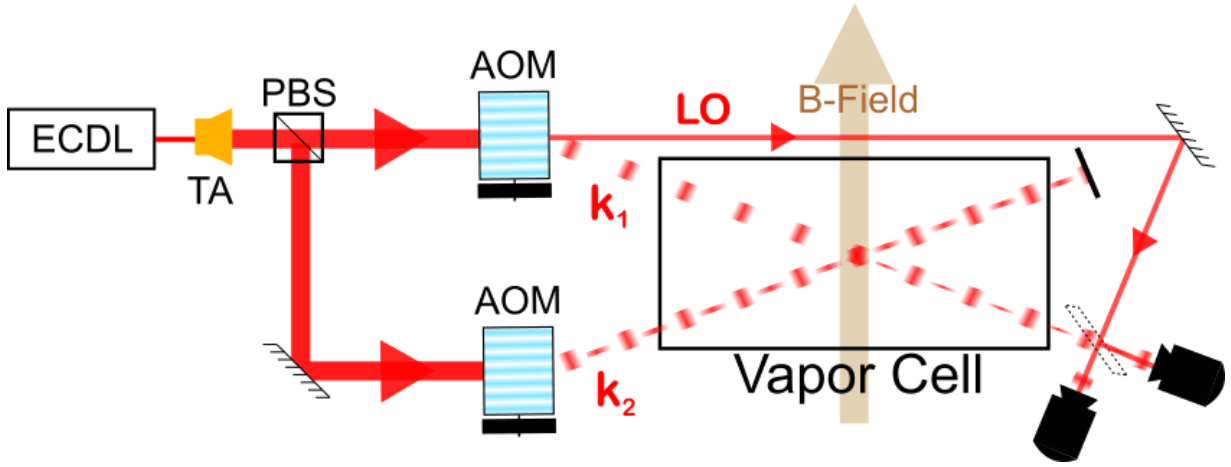

Figure 1. Schematic of the coherence magnetometer.

Figure 1 shows a schematic of a "coherence" magnetometer. Here, a spatially modulated coherence grating is created between adjacent magnetic sublevels of the ground state in Rb vapor by an excitation pulse that consists of two perpendicular linear-polarized traveling waves, with wave vectors $\overrightarrow{k_1}$ and $\overrightarrow{k_2}$, aligned at a small angle θ (a few mrad). The grating is formed along the direction $\overrightarrow{\Delta k} = \overrightarrow{k_1} - \overrightarrow{k_2}$ as shown in Fig. 2 and has a spatial periodicity of $\sim \lambda/\theta$, where $\lambda = 2\pi/k$ and k is the magnitude of the wave vector $k = |\overrightarrow{k_1}| = |\overrightarrow{k_2}|$. The grating can be detected by applying a read-out pulse along the direction $\overrightarrow{k_2}$, and observing the coherent emission scattered along the phase-matched direction $\overrightarrow{k_1}$. This signal, called the magnetic grating free induction decay (MGFID)[15] exhibits a Gaussian decay with a time constant $\tau = 2/ku\theta$, where u is the most probable speed associated with the Maxwell-Boltzmann velocity distribution. This decay corresponds to the thermal motion of atoms causing the grating to dephase. The scattered electric field from the grating is then given by

$$E(t) = E_0 e^{-\left(\frac{ku\theta}{2}\right)^2 t^2} \tag{1}$$

In the presence of a magnetic field, the functional form of the coherence can have a complicated dependence, parametrized by the Larmor frequency. This behavior has been described in Refs. 9 and 10, based on the formalism presented in Ref. 16. While Eq. 1 assumes the thermal trajectory of the atoms is uninterrupted over the length scale of the grating, in the presence of a high concentration of buffer gas the mean-free path of Rb atoms is reduced by collisions and may become much less than the grating spacing. In this limit, the motion of Rb atoms becomes a random walk that can be modeled by the diffusion equation[13]. This condition is represented by

$$\frac{\delta u}{\Gamma_{Col}} \ll \frac{1}{k\theta} \tag{2}$$

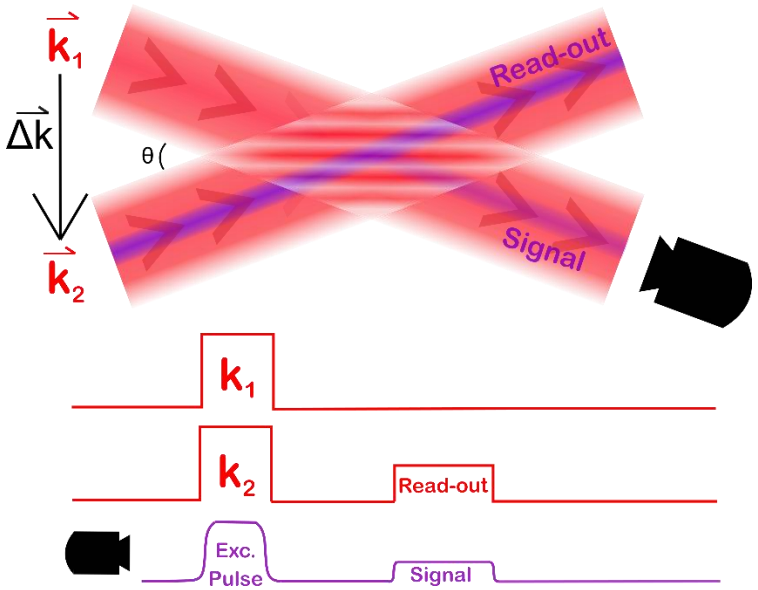

Figure 2: Upper figure shows directions of the excitation pulses, read--out pulse, and signal. The lower figure shows the relative timing of the pulse envelopes along $\overrightarrow{k_1}$ and $\overrightarrow{k_2}$ and the signal envelopes recorded on the detector.

Here, δu is the average velocity change per collision and is the effective collisional rate. When Eq. 2 is satisfied, the evolution of the ground-state density matrix ρ can be described by the diffusion equation,

$$\frac{\partial \rho(x,t)}{\partial t} = -D\nabla^2 \rho(x,t). \tag{3}$$

Here, D is the diffusion coefficient, which is inversely proportional to the perturber pressure. D can be accurately converted to its value at atmospheric pressure D_0, using the relationship $D_0 P_0 = DP$. Here, P_0 is atmospheric pressure and P is the buffer gas pressure in the experiment[17,18]. If the x axis is along $\overrightarrow{\Delta k}$, the spatial dependence of the coherence ρ may be written as $e^{ik\theta x}$. This results in

$$\frac{\partial \rho(x,t)}{\partial t} = -(\theta k)^2 D\rho(x,t) \tag{4}$$

The solution to Eq. 4 is a decaying exponential with a time constant $(k\theta)^2 D$. The MGFID is therefore given by

$$E(t) = E_0 e^{-(\theta k)^2 Dt} \tag{5}$$

Under these conditions, the coherent scattering from the grating is preserved but the signal exhibits an exponential decay with a characteristic time constant $\tau = 1/(D(k\theta)^2)$. Since $(k\theta)^{-1}$ represents the characteristic length scale in this problem, namely the grating spacing, the scaling law for τ is representative of a random walk. Therefore, the coherence magnetometer offers a direct approach for measuring diffusion rates. However, this method is prone to inaccuracies since the scattered signal has a small amplitude and is sensitive to magnetic field gradients.

As a result, we have exploited an interesting aspect of the lin-perp-lin excitation, namely that it simultaneously produces a density grating due to optical pumping. This grating has the same spatial period as the coherence grating. Accordingly, we are able to record decays with much improved signal-to-noise ratios and with greater accuracy due to the insensitivity of the density grating to magnetic fields and field gradients. It should be noted that the density gratings used in this work can be modeled without atomic recoil or matter-wave interference effects[19]. By recording the decay time as a function of angle, we rely on Eq. 5 to measure the diffusion coefficient with a statistical uncertainty of 1%.

4. RESULTS AND DISCUSSION

With reference to the experimental setup described in Fig. 1, we use an ALS described in Ref. 1 and waveguide amplifier system described in Ref. 2 to produce the excitation laser beams. The excitation pulses are amplitude modulated using acousto-optic modulators driven by delay generators with time bases slaved to a rubidium atomic clock. The signal detection is accomplished using a balanced heterodyne arrangement described in Ref. 3. The experiments were carried out in isotopically pure ^{87}Rb vapor in a sealed reference cell containing nitrogen buffer gas. The cell length was 10 cm and it was maintained at 50°C. The decay time, τ of the population grating, was measured as a function of θ to obtain D. As expected, τ was verified to scale as $1/\theta^2$, which is the definitive signature of diffusion. The pressure in the cell was independently determined by measuring the pressure broadened and shifted absorption spectrum as described in Ref. 3.

Table 1 summarizes representative values of the Rb-N_2 diffusion coefficient. The smallest uncertainty prior to this work was achieved by Ref. 20 (2.5%). The discrepancy between measurements utilizing different techniques emphasizes the necessity of a variety of methods, subject to different systematic effects, in arriving at a more reliable value of D_0. Additionally, accurate measurements of the diffusion coefficient constrain theoretical models of many particle systems.

Table 1: Representative measurements of the Rb-N_2 diffusion coefficient at atmospheric pressure D_0. Uncertainties are provided where available.

Reference	**Technique**	$\boldsymbol{D_0}$ $(\mathbf{cm^2/s})$	$\boldsymbol{D_0}$ **rescaled to 50°C**[a] $(\mathbf{cm^2/s})$
Wasghul et al.[21]	Optical pumping relaxation	0.28 at 150°C	0.19
Zeng et al.[22]	Optical pumping relaxation	0.20 at 70°C	0.18
Ishikawa et al.[20]	Magnetic resonance echo	0.159 ± 0.004 at 60°C	0.152 ± 0.004
Franz et al.[23]	Optical pumping relaxation	0.16 at 32°C	0.18
Erickson[24]	Optical pumping relaxation	0.30 at 180°C	0.18
This work[3]	Dephasing of density grating	0.1819 ± 0.0024 at 50°C	0.1819 ± 0.0024

[a]Rescaled using $D \propto T^{3/2}$ [17,18]

5. CONCLUSION

We have demonstrated a distinctive and accurate measurement of the diffusion coefficient of Rb in N_2 relevant to magnetometry. Ideally, the systematic effect due to the N_2 concentration should be measured at buffer gas concentrations of several atmospheres so that spectra can be fit to a smooth lineshape. Since the buffer gas pressure in our isotopically purified rubidium cell could not be changed, we fit the pressure-broadened spectrum to a function appropriate for our pressure range in which the hyperfine features are partially resolved. From Table 1, we note that our measurement disagrees with the previous most precise measurement obtained using spin echoes[20]. Although the diffusion coefficients measured by modeling optical pumping curves[21-24] are in good agreement with our results, we note that these measurements do not report error bounds. However, our determination appears to settle large discrepancies in previously reported values using different techniques. We propose to extend this technique to obtain the most accurate determinations of diffusion coefficients involving buffer gases relevant to Rb vapor magnetometers and a comparative study of the advantages of CMs over traditional time domain magnetometers that rely on the evolution of populations[25]. These measurements will be carried out in a non-magnetic glass manifold in which buffer gas concentrations can be varied and measured independently to corroborate spectroscopy.

6. ACKNOWLEDGEMENTS

We acknowledge a collaboration with Unyob Shim, Sidney Cahn, Andrei Turlapov and Tycho Sleator of New York University. We acknowledge helpful discussions with Louis Marmet of York University and Paul Berman of the University of Michigan. This work was supported by the Canada Foundation for Innovation, the Ontario Innovation Trust, the Ontario Centers of Excellence, the Natural Sciences and Engineering Research Council of Canada (NSERC), and York University.

REFERENCES

[1] Beica, H. C., Pouliot, A., Carew, A., Vorozcovs, A., Afkhami-Jeddi, N., Vacheresse, T., Carlse, G., Dowling, P., Barron, B., and Kumarakrishnan, A., "Characterization and applications of auto-locked vacuum-sealed diode lasers for precision metrology," *Rev. Sci. Inst.* **90**(8), 085113 (2019).

[2] Pouliot, A., Beica, H. C., Carew, A., Vorozcovs, A., Carlse, G., and Kumarakrishnan, A., "Auto-locking waveguide amplifier system for lidar and magnetometric applications," in [*High-Power Diode Laser Technology XVI*], Zediker, M. S., ed., **10514**, 152 – 159, International Society for Optics and Photonics, SPIE (2018).

[3] Pouliot, A., Carlse, G., Beica, H. C., Vacheresse, T., Kumarakrishnan, A., Shim, U., Cahn, S. B., Turlapov, A., and Sleator, T., "Accurate determination of an alkali-vapor–inert-gas diffusion coefficient using coherent transient emission from a density grating," *Phys. Rev. A* **103**, 023112 (Feb 2021).

[4] Allred, J. C., Lyman, R. N., Kornack, T. W., and Romalis, M. V., "High-sensitivity atomic magnetometer unaffected by spin-exchange relaxation," *Phys. Rev. Lett.* **89**, 130801 (Sep 2002).

[5] Suter, D., Rosatzin, M., and Mlynek, J., "Optically driven spin nutations in the ground state of atomic sodium," *Phys. Rev. A* **41**, 1634–1644 (Feb 1990).

[6] Möller, H. E., Chen, X. J., Saam, B., Hagspiel, K. D., Johnson, G. A., Altes, T. A., de Lange, E. E., and Kauczor, H.-U., "MRI of the lungs using hyperpolarized noble gases," *Magnetic Resonance in Medicine* **47**(6), 1029–1051 (2002).

[7] Patil, S. H., "Adiabatic potentials for alkali-inert gas systems in the ground state," *The Journal of Chemical Physics* **94**(12), 8089–8095 (1991).

[8] Higbie, J. M., Rochester, S. M., Patton, B., Holzlöhner, R., Bonaccini Calia, D., and Budker, D., "Magnetometry with mesospheric sodium," *Proc. Natl. Acad. Sci. USA* **108**, 3522–3525 (2011).

[9] Chan, I., Andreyuk, A., Beattie, S., Barrett, B., Mok, C., Weel, M., and Kumarakrishnan, A., "Properties of magnetic sublevel coherences for precision measurements," *Phys. Rev. A* **78**, 033418 (Sep 2008).

[10] Kumarakrishnan, A., Cahn, S. B., Shim, U., and Sleator, T., "Magnetic grating echoes from laser-cooled atoms," *Phys. Rev. A* **58**, R3387–R3390 (Nov 1998).

[11] Kumarakrishnan, A., Shim, U., Cahn, S. B., and Sleator, T., "Ground-state grating echoes from Rb vapor at room temperature," *Phys. Rev. A* **58**, 3868–3872 (Nov 1998).

[12] Tonyushkin, A., Kumarakrishnan, A., Turlapov, A., and Sleator, T., "Magnetic coherence gratings in a high-flux atomic beam," *The European Physical Journal D* **58**, 39–46 (May 2010).

[13] Berman, P. R., "Collisional decay and revival of the grating stimulated echo," *Phys. Rev. A* **49**, 2922–2932 (Apr 1994).

[14] Rothberg, L. J. and Bloembergen, N., "High-resolution four-wave light-mixing studies of collision-induced coherence in Na vapor," *Phys. Rev. A* **30**, 820–830 (Aug 1984).

[15] Berman, P. R. and Dubetsky, B., "Magnetic grating free induction decay and magnetic grating echo," *Laser Physics* **4**, 1017–1029 (1994).

[16] Shore, B., [*The Theory of Coherent Atomic Excitation, 2 Volume Set*], Wiley (1990).

[17] Chapman, S., Cowling, T., and D., B., [*The Mathematical Theory of Non-uniform Gases: An Account of the Kinetic Theory of Viscosity, Thermal Conduction and Diffusion in Gases*], Cambridge University Press, 3 ed. (1990).

[18] Cussler, E. L., [*Diffusion: Mass Transfer in Fluid Systems*], Cambridge Series in Chemical Engineering, Cambridge University Press, 3 ed. (2009).

[19] Barrett, B., Carew, A., Beica, H. C., Vorozcovs, A., Pouliot, A., and Kumarakrishnan, A., "Prospects for precise measurements with echo atom interferometry," *Atoms* **4**(3), 19–61 (2016).

[20] Ishikawa, K. and Yabuzaki, T., "Diffusion coefficient and sublevel coherence of Rb atoms in N_2 buffer gas," *Phys. Rev. A* **62**, 065401 (Nov 2000).

[21] Wagshul, M. E. and Chupp, T. E., "Laser optical pumping of high-density Rb in polarized ^{3}He targets," *Phys. Rev. A* **49**, 3854–3869 (May 1994).

[22] Zeng, X., Wu, Z., Call, T., Miron, E., Schreiber, D., and Happer, W., "Experimental determination of the rate constants for spin exchange between optically pumped K, Rb, and Cs atoms and ^{129}Xe nuclei in alkali-metal–noble-gas van der Waals molecules," *Phys. Rev. A* **31**, 260–278 (Jan 1985).

[23] Franz, F. A. and Sooriamoorthi, C. E., "Analytic expressions for transient signals in the optical pumping of alkali-metal vapors," *Phys. Rev. A* **8**, 2390–2401 (Nov 1973).

[24] Erickson, C. J., PhD dissertation, Princeton University (2000).

[25] Chan, I., Barrett, B., and Kumarakrishnan, A., "Precise determination of atomic *g*-factor ratios from a dual isotope magneto-optical trap," *Phys. Rev. A* **84**, 032509 (Sep 2011).